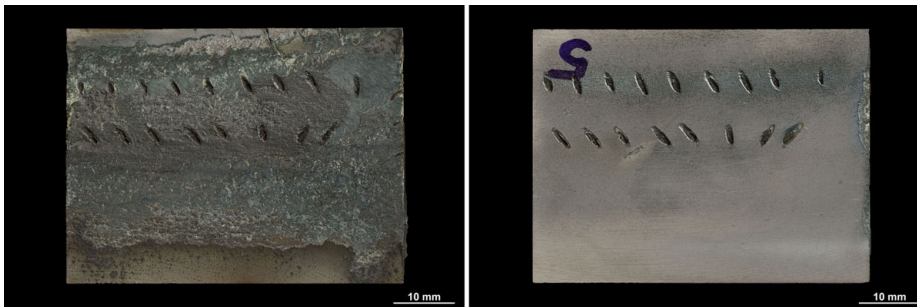




## Executive summary

# Service experience with single crystal superalloys for high pressure turbine shrouds


**Report no.**

NLR-TP-2011-547

**Author(s)**
T.J. Nijdam  
R van Gestel
**Report classification**

UNCLASSIFIED

**Date**

December 2010

**Knowledge area(s)**

Gasturbinetechnologie

**Descriptor(s)**
Superalloys  
Single Crystals  
Shrouds  
Field experience
**Problem area**

Chromalloy Holland delivers repaired, modified or new (PMA-parts) high pressure turbine (HPT) shrouds to the maintenance shops of airliners as an alternative to the parts delivered by the original equipment manufacturer (OEM) for various aero and aero derivative gas turbine engines.

During engine operation, the HPT shrouds are exposed to very high temperatures and aggressive environments. In addition, the blade tips may contact the shroud gas path surface (e.g. during a hard landing), a phenomenon further referred to as rubbing. Both phenomena may lead to a severe deterioration of the shroud up to the point where the airliners have to remove the shrouds from the engine in order to replace or repair them.

Knowledge of the type and extent of service degradation occurring for

HPT shrouds is of prime importance for Chromalloy Holland, since this information can act as valuable input for making improved shroud designs and selecting improved shroud materials.

**Description of work**

Therefore, during the last 10 years, Chromalloy Holland and NLR have started classifying the various forms of service-induced damage that are observed for HPT shrouds as function of the engine type. In this paper, the main results from these investigations are summarized. This overview will mainly discuss the service experiences with HPT shrouds in the hot section of the CFM56, CF6-50 and CF6-80C2 aero engines.

**Results and conclusions**

It is shown that uncoated single crystal superalloy HPT shrouds primarily degrade by environmental attack. Depending on the engine

This report is based on a presentation held at the 5th International Gas Turbine Conference: "The Future of Gas Turbine Technology", Brussels, Belgium, 27-28 October 2010.

type, type I hot corrosion or oxidation accelerated by rubbing is the most dominant degradation mode.

Single crystal superalloy CMSX-4 and René N5 CFM56-5C shrouds are primarily attacked by oxidation. However, severe oxidation attack only occurs when the shroud also experiences shroud-to-blade-tip rubbing. If no rubbing occurs during engine operation, the degree of oxidation attack is minimal.

1<sup>st</sup> stage single crystal superalloy CMSX-4 and René N5 shrouds for the CF6-80C2 engine either are attacked by oxidation or type I hot corrosion. In general, the degree of environmental attack for CF6-80C2 shrouds is much less than for the

CFM56-5C shrouds and the CF6-50 shrouds.

1<sup>st</sup> stage CF6-50 shrouds made out of the single crystal superalloy N2 show severe environmental attack despite the fact that N2 has been specifically developed for optimum oxidation and hot corrosion resistance.

Rub coatings that are applied during repair of single crystal superalloy HPT shrouds are less prone to environmental degradation, but are susceptible to cracking around cooling holes and coating spallation near corners and edges.

#### **Applicability**

Single crystal superalloy high pressure turbine shrouds in aero-engines and aero derivative industrial gas turbines.



NLR-TP-2011-547

## Service experience with single crystal superalloys for high pressure turbine shrouds

T.J. Nijdam and R van Gestel<sup>1</sup>

<sup>1</sup> Chromalloy Holland

This report is based on a presentation held at the 5th International Gas Turbine Conference: "The Future of Gas Turbine Technology", Brussels, Belgium, 27-28 October 2010.

The contents of this report may be cited on condition that full credit is given to NLR and the authors.  
This publication has been refereed by the Advisory Committee AEROSPACE VEHICLES.

Customer	National Aerospace Laboratory NLR
Contract number	---
Owner	NLR
Division NLR	Aerospace Vehicles
Distribution	Unlimited
Classification of title	Unclassified
	December 2011

Approved by:

Author  T.J. Nijdam 07/12/11	Reviewer  E. Amsterdam 07-12-11	Managing department 
---	---	--





## Summary

Knowledge of the type and extent of service degradation occurring for high pressure turbine (HPT) shrouds in aero-engines and aero derivative industrial gas turbines is of prime importance to develop improved shroud designs and materials. In this paper, an overview is given of the service experiences with HPT shrouds in the hot section of the CFM56, CF6-50 and CF6-80C2 aero engines. This information is part of on-going investigations at Chromalloy Holland and NLR to classify the service damage modes of HPT shrouds in different engines. It is shown that uncoated CMSX-4 and René N5 single crystal superalloy shrouds primarily degrade by means of rub-enhanced oxidation (CFM56 engines) and/or hot corrosion (CF6-80C2 engines). Mechanical damage e.g. in the form of cracking is rarely observed. A recently introduced hot corrosion resistant superalloy N2 is also severely corroded upon service in CF6-50 engines. Single crystal superalloy shrouds with an external rub coating are less prone to oxidation and hot corrosion, but are susceptible to coating spallation and cracking around cooling holes.

## Contents

<b>1</b>	<b>Introduction</b>	<b>7</b>
<b>2</b>	<b>Materials and properties</b>	<b>8</b>
<b>3</b>	<b>Service Experience</b>	<b>16</b>
3.1	CMSX-4 and René N5 CFM56-5C shrouds	17
3.2	CMSX-4 and René N5 CF6-80C2 shrouds	21
3.3	N2 CF6-50 shrouds	25
3.4	René N5 shrouds with TDC coating	27
<b>4</b>	<b>Discussion</b>	<b>29</b>
<b>5</b>	<b>Conclusions</b>	<b>32</b>
	<b>Acknowledgements</b>	<b>32</b>
	<b>References</b>	<b>33</b>



## Abbreviations

CSO	Cycles Since Overhaul
EDS	Energy Dispersive Spectroscopy
HPT	High Pressure Turbine
HVOF	High Velocity Oxygen Fuel
IGT	Industrial Gas Turbine
LCF	Low Cycle Fatigue
LOM	Light Optical Microscopy
LMP	Larson Miller Parameter
LPPS	Low Pressure Plasma Spraying
NLR	National Aerospace Laboratory
OEM	Original Equipment Manufacturer
PMA	Parts Manufacturing Approval
SEM	Scanning Electron Microscopy
TDC	Thermally Densified Coating
TSO	Time Since Overhaul



This page is intentionally left blank.

## 1 Introduction

High pressure turbine (HPT) shrouds, which are used to minimize the leakage of air around the turbine blade tips, are valuable components in aero-engines and industrial gas turbines (IGTs) to improve engine efficiency and performance. The shrouds can be of various designs and be produced with various materials, depending on the engine type and the engine original equipment manufacturer (OEM). The present paper is concerned with the HPT shrouds that are used in the CF6-50, CF6-80C2, CF34-3B1, CFM56-2/3, CFM56-5B/7B and CFM56-5C aero-engines and the LM5000 and LM6000 aero-derivative gas turbine engines. For these engines, Chromalloy Holland delivers repaired, modified or new (PMA-parts) HPT shrouds to the maintenance shops of airlines as an alternative to the parts delivered by the OEM (General Electric). An example of such a HPT shroud is shown in Fig. 1. Each shroud is made of solid metal and contains a smooth gas path surface. During engine operation, the hot gasses pass over this surface along the axial direction from the forward to the aft side of the shroud. Simultaneously, the turbine blade tips pass the shroud's surface along the circumferential direction. Each turbine stage contains a multiple amount of these shrouds (the exact number depends on the engine type), which are placed side by side along the circumferential direction to form a complete sealing ring. Most of the shrouds contain cooling holes to provide film cooling at the shroud's gas path surface. The location and amount of these cooling holes are considered important design parameters to control the temperature and stress distribution in the shrouds during engine operation.

During engine operation, the HPT shrouds are exposed to very high temperatures (there are few components in an engine that experience similar or higher temperatures) and aggressive environments. In addition, the blade tips may contact the shroud gas path surface (e.g. during a hard landing), a phenomenon further referred to as blade tip-to-shroud rubbing or simply rubbing. Both the exposure to high temperatures and the rubbing events may lead to a severe deterioration of the shroud up to the point where the airlines have to remove the shrouds from the engine in order to replace or repair them.

Knowledge of the type and extent of service degradation occurring for HPT shrouds is of prime importance for Chromalloy Holland, since this information can act as valuable input for making improved shroud designs and selecting improved shroud materials. Therefore, during the last 10 years, Chromalloy Holland has started classifying the various forms of service-induced damage that are observed for HPT shrouds as function of the engine type. Parts of these investigations were performed by Chromalloy Holland; the other investigations were carried out at the National Aerospace Laboratory (NLR) in close cooperation with Chromalloy. In this paper, the

main results from these investigations are summarized. This overview will mainly discuss the service experiences with HPT shrouds in the hot section of the CFM56, CF6-50 and CF6-80C2 aero engines.

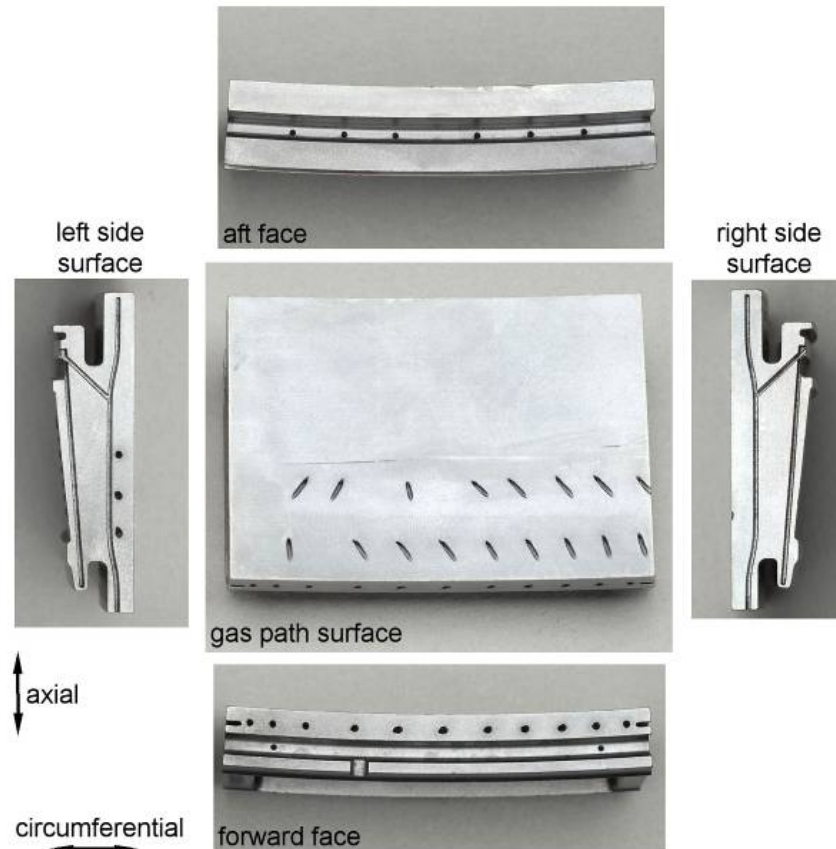


*Fig. 1: Macrographs of a CFM56-5C shroud recorded along different directions (the back surface is not shown). The hot gasses flow from the forward to the aft face over the shroud's gas path surface.*

## 2 Materials and properties

In order to develop a better understanding of the different degradation modes for HPT shrouds, it is instructive to first examine what kind of materials are used for HPT shrouds and what kind of characteristic properties they have. Figs. 2 and 3 illustrate the material use history for HPT shrouds in the various aero-engines considered in this paper. The material use history for the aero-derivative engines is not shown, but it should be noted that the LM5000 shrouds are the same as the shrouds for the CF6-50 engine and the LM6000 shrouds are the same as the shrouds for the CF6-80C2 engine. It is seen that the following substrate materials have been used by the OEM and Chromalloy Holland: Hastelloy X, René 41, René 77, MAR-M509, René N5, CMSX-4, N2 and N500. The chemical compositions of these alloys are listed in Table 1.

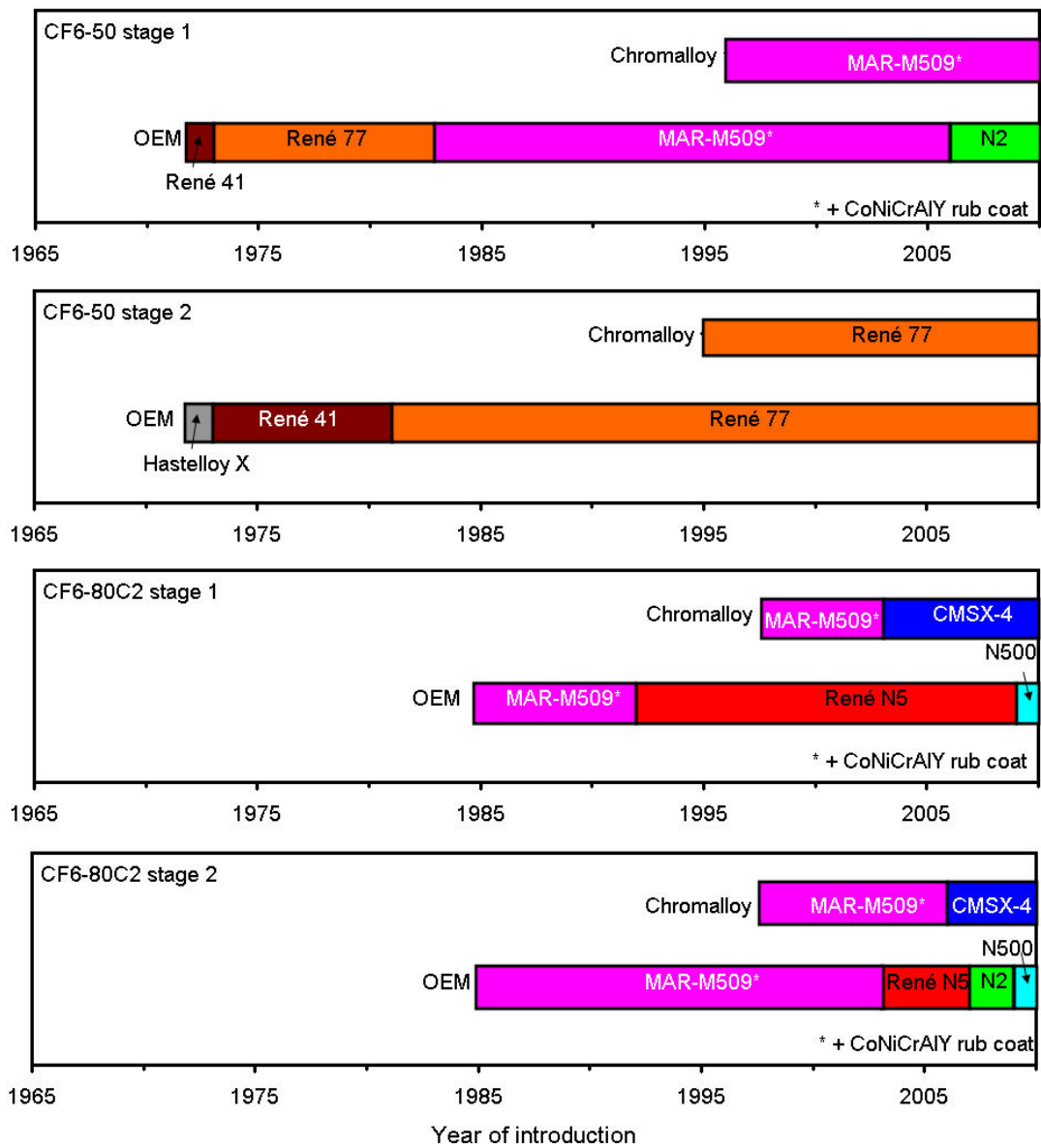


Fig. 2: History of material use for HPT shrouds in the CF6-50 and CF6-80C2 aero-engines. Information provided by Chromalloy.

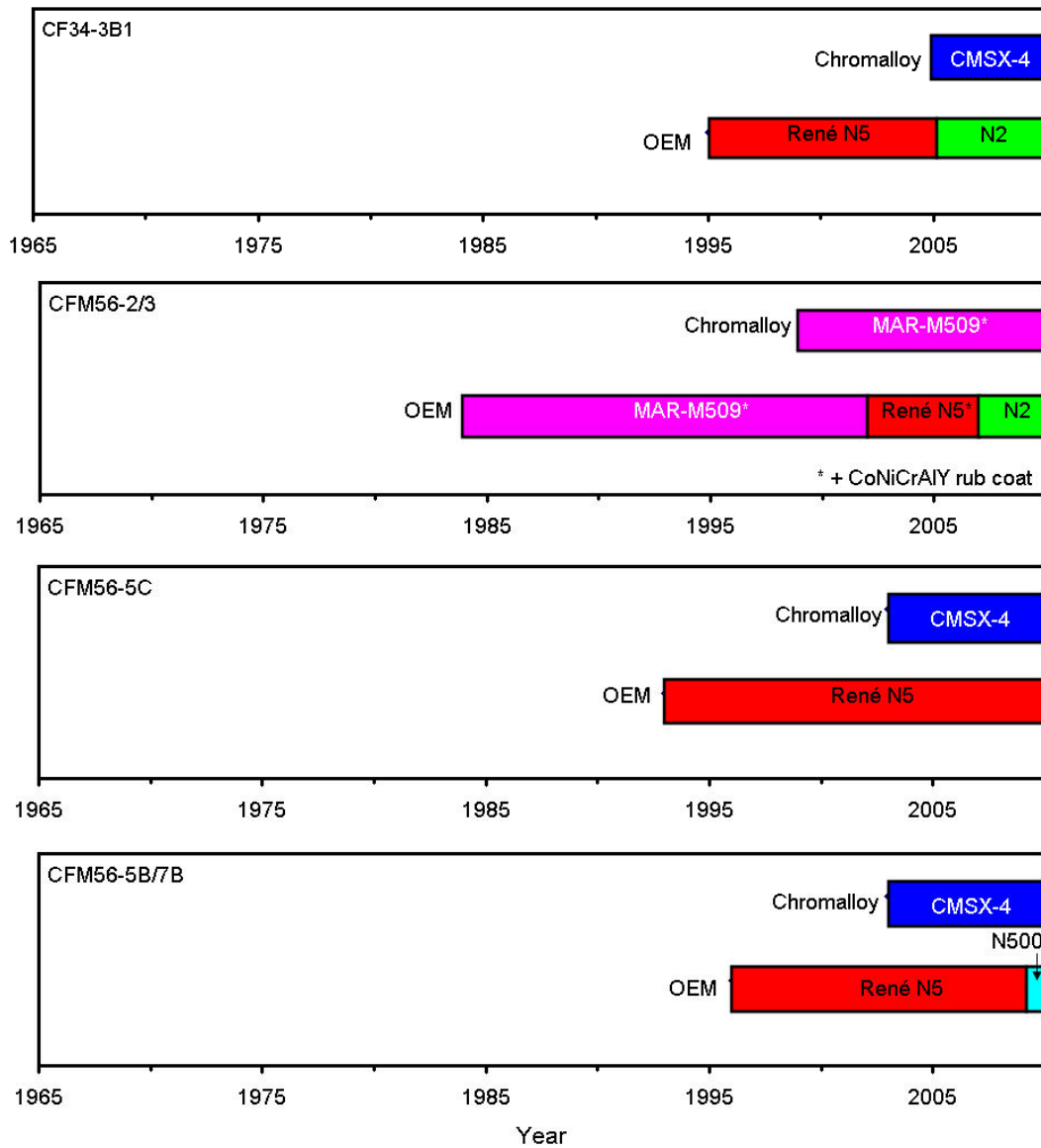


Fig. 3: History of material use for HPT shrouds in the CF34-3B1, CFM56-2/3, CFM56-5C and CFM56-5B/7B aero-engines. Information provided by Chromalloy.

Table 1: Nominal chemical compositions (in wt%) of the substrate materials used for CF6-50, CF6-80C2, CF34-3B1 and CFM56 HPT shrouds. Sources: Refs. [1-4].

	Ni	Cr	Co	Mo	Re	W	Al	Ti	Ta	Hf	Other
Hastelloy X [1]	Bal.	22	1.5	9		0.6	2.0				Fe,C
René 41 [1]	Bal.	19	11	10			1.5	3			C
René 77 [1]	Bal.	15	15	4.2			4.3	3.3			C,B,Zr
MAR-M509 [1]	10	24	Bal.	-		7		-	3.5		C
René N5 [2]	Bal.	7	8	2	3	5	6.2		6	0.2	C,Y
CMSX-4 [2]	Bal.	6.5	9	0.6	3	6	5.6	1	6.5	0.1	
N2 [3]	Bal.	13	7.5	-	1.6	3.8	6.6		5	0.2	
N500 [4]	Bal.	6	7.5	2		6	6.2		6.5	0.6	C,B

It is seen that for the oldest engine (CF6-50), the first OEM shrouds were made out of the wrought nickel base superalloys Hastelloy X and René 41. However, these materials were soon replaced by the cast nickel base superalloy René 77 by the OEM. During the 1980s, this alloy was replaced with the polycrystalline Co base superalloy MAR-M509. MAR-M509 was subsequently also introduced in other engines. MAR-M509 has been used for a relatively long time by the OEM and is still being used in some engines today.

During the 1990s, the first single crystal superalloy shrouds were introduced in new engines (e.g. CFM56-5C and CFM56-5B/7B) and in some of the older engines (CF6-80C2). The single crystal shrouds were cast with their growth direction (i.e. the <001> crystallographic direction) parallel to the circumferential direction of the shroud using the proprietary 2<sup>nd</sup> generation (3 wt% Re) single crystal superalloy René N5. Chromalloy has responded to this by introducing the commercially available 2<sup>nd</sup> generation single crystal superalloy CMSX-4 for HPT shrouds in 2003. Recently, the OEM has introduced two new proprietary single crystal superalloys for HPT shrouds. In 2005 / 2006, the Al and Cr-rich single crystal superalloy N2 was introduced [3], mainly in those engines where MAR-M509 was used (see Figs. 2 and 3). In 2009, the new single crystal superalloy N500 was introduced by the OEM, mainly as an alternative to René N5 (see Fig. 2). The particular feature of N500 is its zero Re content [4]. The Re price level has increased dramatically from 2006 to 2010. As a result, the raw material costs for producing CMSX-4 and René N5 HPT shrouds have also increased dramatically.

For the interpretation of the field experiences, it is also important to know that for some HPT shrouds the gas path surface is protected with a rub coating. As seen in Fig. 2, rub coatings are applied during the production and repair of all MAR-M509 shrouds. For the single crystal superalloys (CMSX-4, René N5, N2 and N500) the rub coatings are not applied during

production, i.e. during the first service interval the gas path surface of these shrouds is exposed uncoated to the engine environment. For CMSX-4 and René N5, an external rub coating is employed during repair, but the main reason for this is to compensate for the reduction in the shroud thickness that occurs when service damage is removed during repair. With respect to the rub coatings, the OEM and Chromalloy distinguish their selves mainly from each other by means of the coating composition (see Table 2) and the way in which the coatings are applied. Chromalloy uses a CoNiCrAlY rub coating both for MAR-M509 and single crystal superalloy shrouds. This coating was deposited by means of low pressure plasma spraying (LPPS) for many years, but recently Chromalloy has switched to high velocity oxygen fuel (HVOF) spraying. The OEM uses both HVOF rub coatings and so-called thermally densified coatings (TDCs). Currently, the OEM uses three different coating compositions (see Table 2): (1) a CoNiCrAlY coating only used for MAR-M509 shrouds, (2) a NiCoCrAlY coating used for repair of single crystal superalloy shrouds, and (3) a René 195 TDC used for repair of single crystal superalloy shrouds that need to perform for very long service times under the most aggressive conditions [5].

*Table 2: Nominal chemical compositions (in wt%) of the rub coatings used for CF6-50, CF6-80C2, CF34-3B1 and CFM56 HPT shrouds. Source: Ref. [5].*

	Ni	Co	Cr	Al	Ta	W	Re	Si	Y	Hf
CoNiCrAlY TDC [5]	34	Bal.	22.	7				3.3	0.05	
CoNiCrAlY HVOF	32	Bal.	21	8					0.5	
NiCoCrAlY TDC [5]	Bal.	15	20	7.8				2.5	0.05	
René 195 TDC [5]	Bal.	5.6	10.2	7.2	4.3	3.1	1.3	2.1		0.1

The characteristic properties of the superalloys considered in this work are shown in Figs. 3 to 6 with MAR-M509 chosen as the baseline reference material to which all other materials are compared. These property data were either obtained from literature or determined by means of laboratory mechanical and environmental tests at NLR.

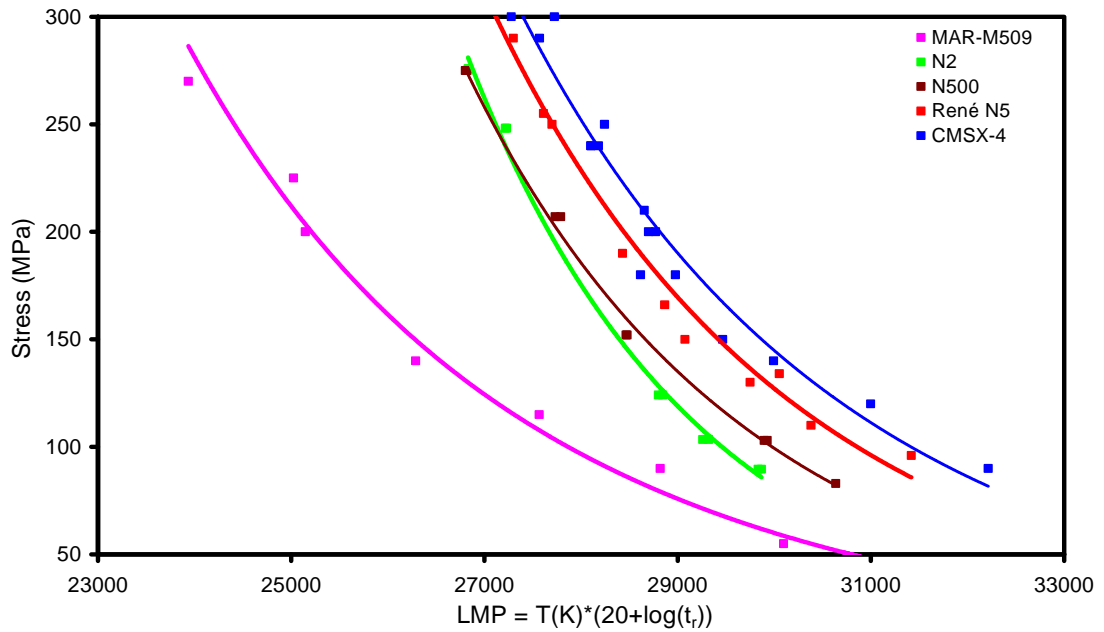


Fig. 3: Creep resistance of MAR-M509 [1], N2 [3], N500, CMSX-4 [6] and René N5 [7]. The creep life is plotted as function of the Larson-Miller Parameter (LMP), which includes the time ( $t_r$ ) at which rupture occurs at a testing temperature  $T$  and applied stress level  $\sigma$ .

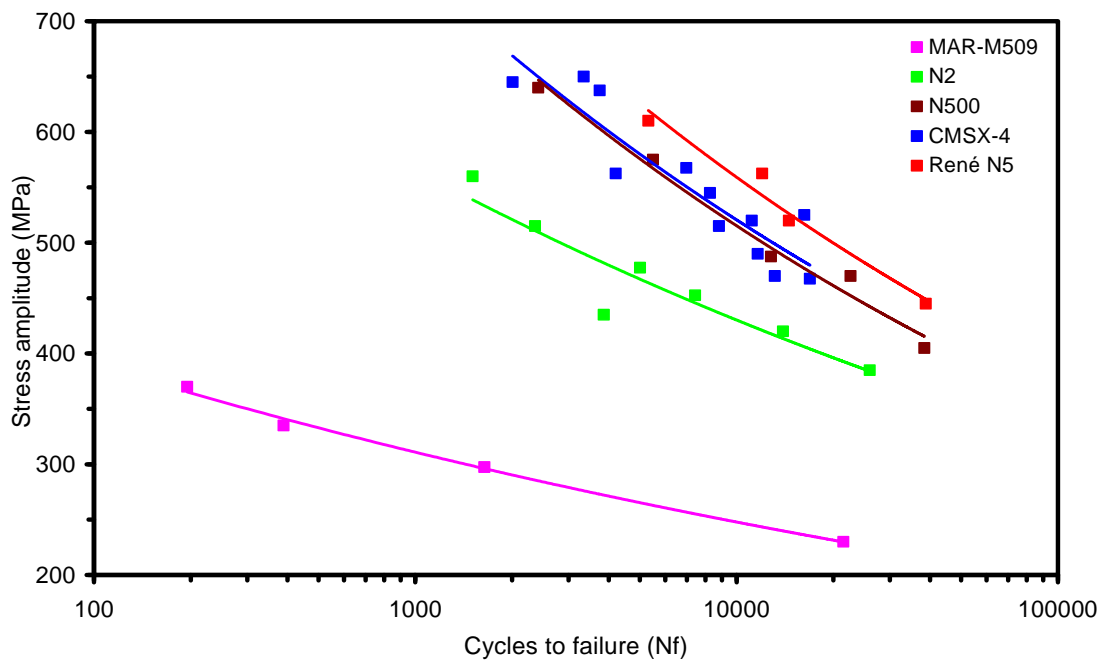


Fig. 4: Low cycle fatigue resistance of MAR-M509, N2, N500, CMSX-4 and René N5 at a temperature of 850 °C and an R ratio of 0.05. The LCF life is plotted as function of the stress amplitude at half life.

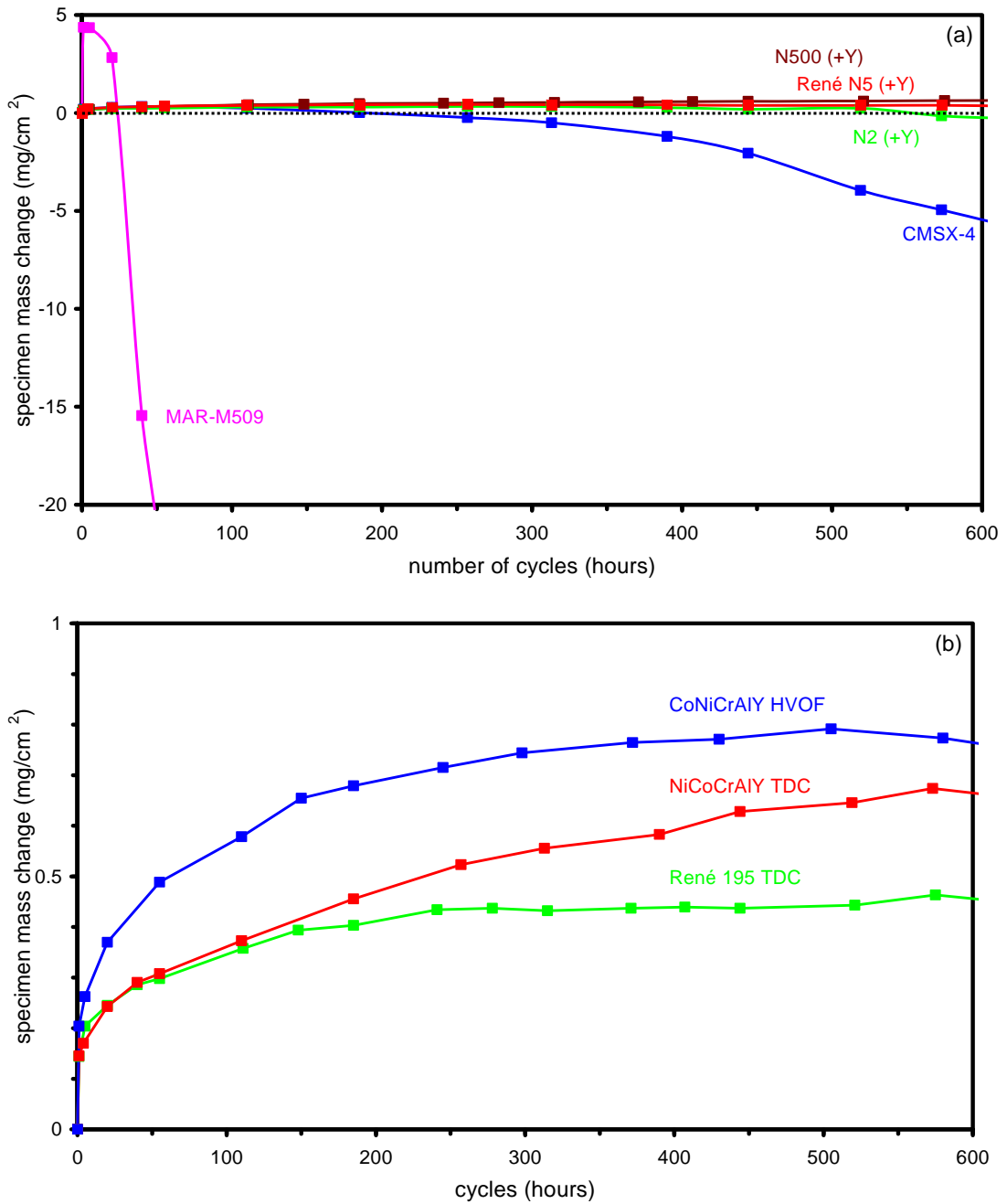


Fig. 5: cyclic oxidation resistance of (a) the substrate materials MAR-M509, N2, N500, CMSX-4 and René N5 and (b) the rub coatings CoNiCrAlY HVOF, NiCoCrAlY TDC and René 195 TDC at 1093 °C (1 h cycles).

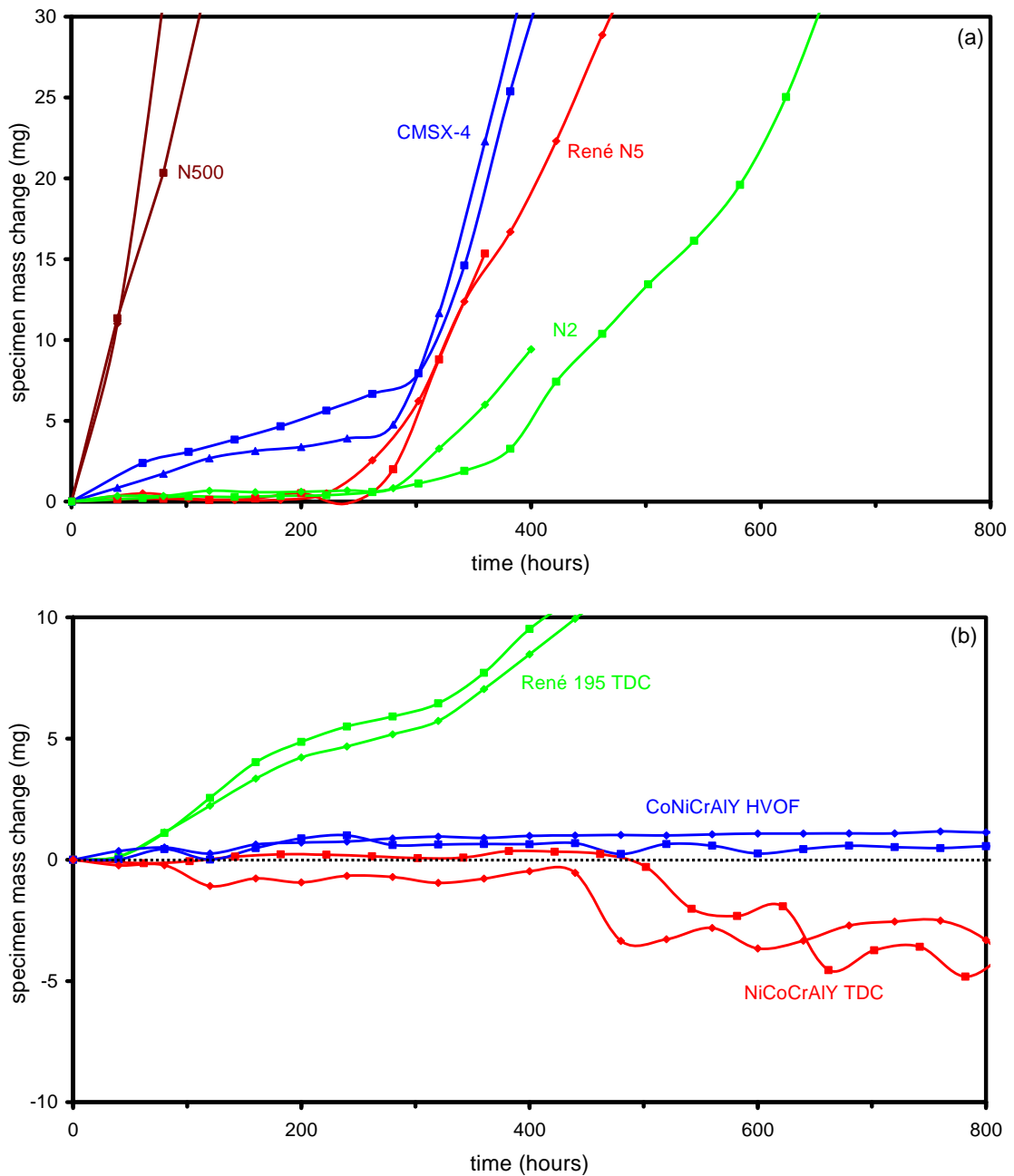


Fig. 6: Type I hot corrosion resistance of (a) substrate materials N2, N500, CMSX-4 and René N5, and (b) rub coatings CoNiCrAlY HVOF, NiCoCrAlY TDC and René 195 TDC at 900 °C.

From Figs. 3 and 4 it is seen that the mechanical properties of all single crystal superalloys are superior to those of MAR-M509, as expected. It is also clear that the recently introduced material N2 was not primarily developed because of its high strength. The creep and LCF properties of N2 are below those of the 2<sup>nd</sup> generation single crystal CMSX-4 and René N5. This may also explain why N2 was not introduced as HPT shrouds in all engines, but only in some older engines which are likely to operate at lower turbine inlet temperatures. The Re free

single crystal superalloy N500 has a lower creep resistance than the 2<sup>nd</sup> generation single crystals CMSX-4 and René N5, but its LCF resistance is quite good (comparable to CMSX-4).

All single crystal superalloys also have superior oxidation resistance compared to MAR-M509. The reasons for this are the absence of grain boundaries (grain boundaries are often preferentially attacked during oxidation) and the relatively high Al content (>5.5 wt%) of CMSX-4, René N5, N500 and N2. The latter permits the formation of a continuous alumina scale which often provides the best oxidation protection [8]. It is also seen that CMSX-4 is more susceptible to oxide spallation than René N5 and N2. It is believed that this is due to the addition of small amounts of Y to René N5, N500 and N2, which are known to improve the oxide scale adherence dramatically [8]. The standard version of CMSX-4 does not contain such small additions of so-called reactive elements (i.e. Y), and is therefore more prone to oxide scale spallation. Finally, it is seen that the single crystal superalloy N500 is highly prone to type I hot corrosion resistance in comparison to other single crystal superalloys (e.g. CMSX-4 and René N5). This is most likely due to the lower Cr content in N500 in comparison to CMSX-4 and René N5. N2 clearly performs better than CMSX-4 and René N5 in a type I hot corrosion test. However, the hot corrosion resistance of N2 is still much poorer than that of a MCrAlY rub coating (compare Figs. 6a and b).

The rub coatings exhibit various combinations of type I hot corrosion and oxidation resistance. The René 195 TDC has the best oxidation resistance, but is relatively poor in hot corrosion resistance. The CoNiCrAlY HVOF rub coating combines excellent hot corrosion resistance with acceptable oxidation resistance. Finally, the hot corrosion and oxidation resistance of the NiCoCrAlY TDC lies in between that of the René 195 TDC and the CoNiCrAlY HVOF coatings.

### **3 Service Experience**

In this section several examples are given of investigations performed on ex-service HPT shrouds. Such ex-service shrouds were sent by airlines to Chromalloy Holland for repair or replacement. Usually, Chromalloy took macrographs from these shrouds when the shrouds entered the repair procedure. In addition, selected shrouds were set aside and reserved for further investigation. Such an investigation typically included the sectioning of the ex-service shroud in the axial direction perpendicular to the gas path surface (Fig. 1) and the subsequent analysis of this cross-section with light optical microscopy (LOM), scanning electron microscopy (SEM) and energy dispersive X-ray spectroscopy (EDS).

### 3.1 CMSX-4 and René N5 CFM56-5C shrouds

Generally speaking, the observable damage to CMSX-4 and René N5 CFM56-5C HPT shrouds is mostly confined to the gas path surface. The appearance of the sets of shrouds that are supplied to Chromalloy can differ significantly. Fig. 7 gives two representative examples. It is seen that one set of shrouds is highly discoloured, indicating severe environmental attack, while the other set of shrouds appears almost completely clean. So far, no systematic relation has been found between the appearance of the shroud gas path surface and the engine service conditions. In other words, no difference has yet been observed for shrouds exposed to long flights (high time since overhaul (TSO) and low number of cycles since overhaul (CSO)) and short flights (low TSO and high CSO). Moreover, frequently, significant differences in the appearance of the shroud surface are observed for shrouds originating from the same set (i.e. from the same engine; see e.g. Fig. 7a).

To examine whether this difference in macroscopic appearance was an indication for a different degree of environmental attack, the shroud that macroscopically appeared to be the most attacked and the shroud that appeared to be the least attacked were analyzed in more detail for the set of shrouds shown in Fig. 7a. The results of this analysis are presented in Figs. 8 and 9. It is seen that, for both shrouds, a very thick (300 – 400  $\mu\text{m}$ ) corrosion product formed at the gas path surface during service. A compositional analysis of the corrosion product revealed that it consisted of a porous continuous upper layer composed of mainly nickel and cobalt oxides and an inner layer composed of isolated internal aluminium and chromium oxides. Hence, in contrast to what is expected based on laboratory cyclic oxidation tests, no continuous alumina scale developed for these shrouds upon service. As a result, the corrosion product is able to rapidly consume the single crystal superalloy shroud. There seems to be no difference in the thickness of the corrosion product for the shroud that appeared to be severely degraded and the shroud that appeared to be less degraded macroscopically. It is therefore believed that the different appearance for shroud 20 (Fig. 8) is related to differences in blade tip rubbing. It is clearly seen that shroud 20 (Fig. 8) exhibited a deeper rub trace than shroud 30 (Fig. 9). As a result, due to this deeper rubbing, part of the corrosion product has been removed away by erosion or spallation (Figs. 8a and 8b). Macroscopically, it therefore appears that shroud 20 is more severely attacked while in reality it is not.

(a) CFM56-5C René N5 (uncoated) ; TSO 28306 ; CSO 3430



(b) CFM56-5C René N5 (uncoated) ; TSO 11616 ; CSO 2257



Fig. 7: Macrographs of two complete sets of CFM56-5C René N5 HPT shrouds (uncoated). The blue inserts show which shrouds were selected for further evaluation.

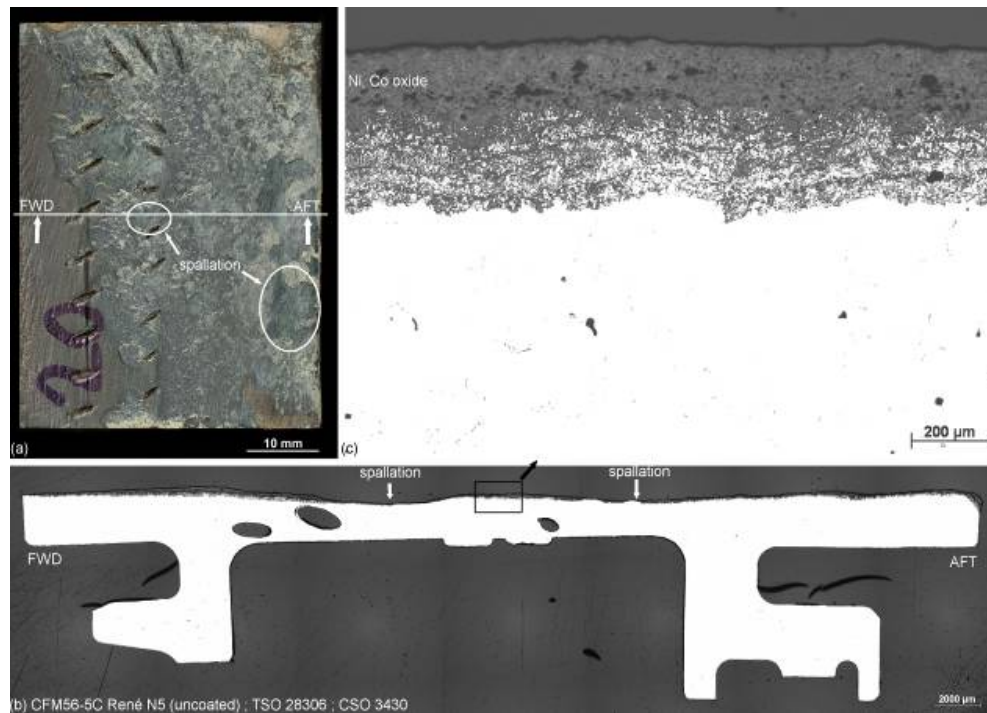


Fig. 8: (a) Surface macrograph, (b) optical micrograph of the cross-section indicated in (a) and (c) optical micrograph of the corrosion product at the location indicated in (b) of an ex-service René N5 CFM56-5C HPT shroud.

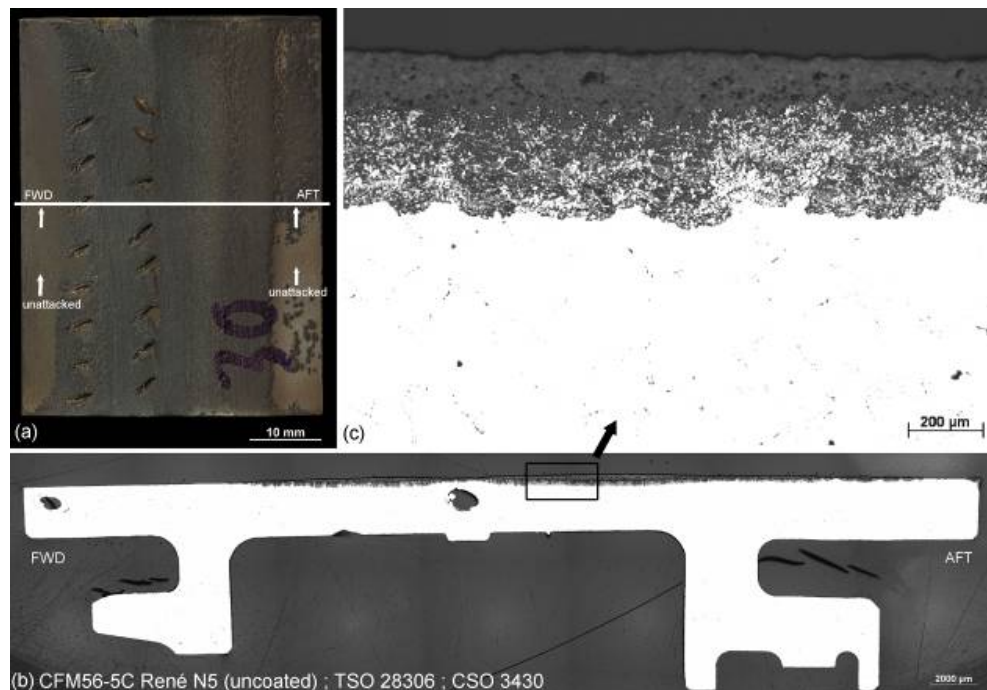
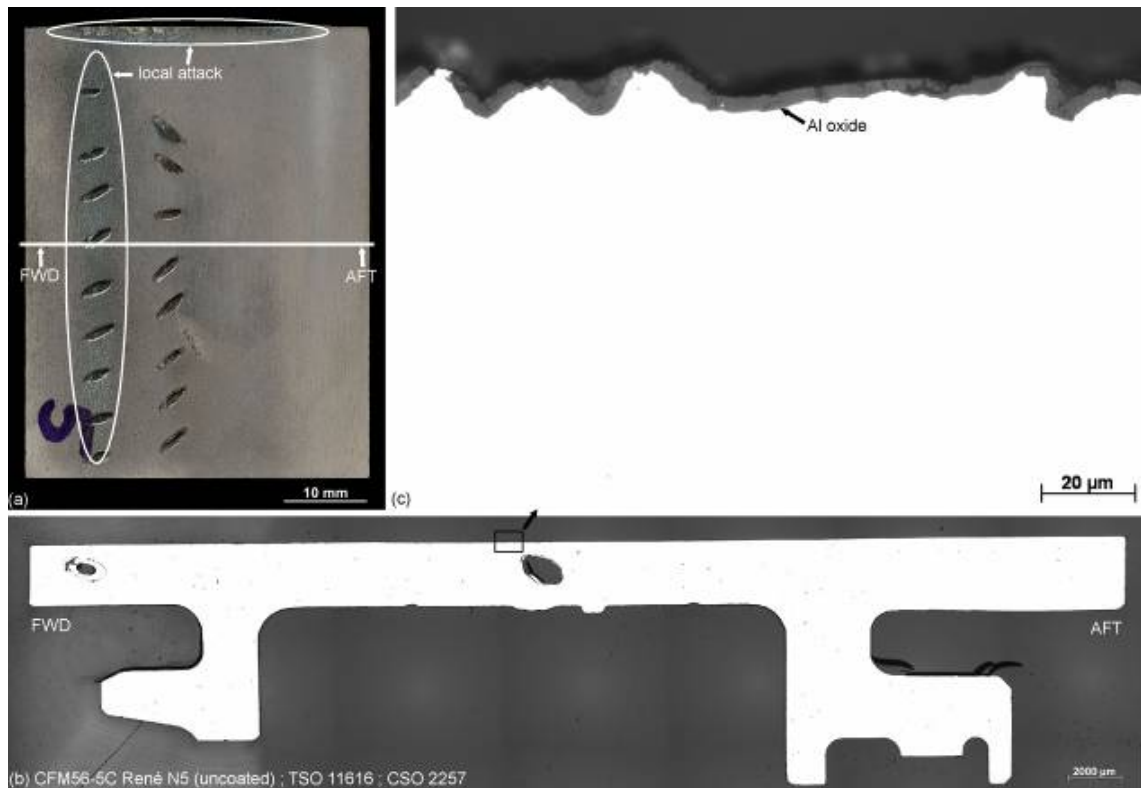


Fig. 9: (a) Surface macrograph, (b) optical micrograph of the cross-section indicated in (a) and (c) optical micrograph of the corrosion product at the location indicated in (b) of an ex-service René N5 CFM56-5C HPT shroud.



*Fig. 10: (a) Surface macrograph, (b) optical micrograph of the cross-section indicated in (a) and (c) optical micrograph of the corrosion product and the location indicated in (b) of an ex-service René N5 CFM56-5C HPT shroud.*

Fig. 10 shows an example of a shroud that appears to be relatively clean after service. An examination of this shroud cross-section revealed that it indeed has not been severely attacked by corrosion. Only a very thin continuous oxide scale ( $2.5 \mu\text{m}$  thick) could be detected upon the gas path surface of this shroud despite its TSO of more than 11.000 hours. Compositional analysis revealed that this oxide layer was composed of aluminium oxide, in agreement with the laboratory furnace tests. It seems highly unlikely that differences in normal engine conditions can explain the huge difference (more than two orders of magnitude difference in oxide thickness) between the environmental attack for the shrouds shown in Figs. 7a and 7b. On closer inspection of Figs. 8 to 10 and other cross-sectioned René N5 and CMSX-4 CFM56-5C shrouds, it seems that the difference in oxidation behaviour can be attributed to rubbing. In the shrouds where rubbing was absent (e.g. Fig. 10) oxidation always proceeded very slowly, in agreement with what is observed in the laboratory. However, in the shrouds which experienced rubbing, the oxidation rate was always much faster. Additional evidence for this explanation can be found on the gas path surface of rubbed shrouds far away from the rub area. As is seen in e.g. Figs. 9a and b, shroud no. 30 does not seem to be environmentally attacked far away from the rub area. Apparently, rubbing only influences a limited area surrounding the rub trace. The

question remains why rubbing does result in such an enhancement of the oxidation rate. One explanation could be that due to rubbing the material temperature at the gas path surface raises to such a high level that a continuous alumina layer cannot be formed anymore. However, such an explanation needs yet to be verified.

### **3.2 CMSX-4 and René N5 CF6-80C2 shrouds**

Typical macrographs from the gas path surface of 1<sup>st</sup> stage CMSX-4 CF6-80C2 HPT shrouds are shown in Fig. 11. Similar to what was observed for the CFM56-5C HPT shrouds, environmental attack seems to be accelerated in the area where rub has occurred on the shroud surface. However, typically, the extent of the environmental attack for the CF6-80C2 shrouds seems to be less than what is usually observed for CFM56-5C shrouds. This was confirmed when a cross-section of one of the CF6-80C2 HPT shrouds was examined in more detail (see Fig. 12). As shown in Fig. 12c, the corrosion product on this shroud had a thickness of only 5 – 10  $\mu\text{m}$ , which is much thinner than what was observed for CFM56-5C shrouds (Figs. 8-10). EDS analysis revealed that the corrosion product in Fig. 12c was made up of three layers: (1) an outer Ni rich oxide layer, (2) an intermediate Ta, W rich oxide layer, and (3) a continuous inner aluminium oxide layer. In addition, Cr-rich sulphides were detected just below the alumina layer. This indicates that this shroud was attacked by type I hot corrosion. Due to the relatively thin corrosion product, it is likely that the hot corrosion reaction was still in its initiation phase after 3402 hours of engine operation.

While type I hot corrosion was observed within other 1<sup>st</sup> stage CMSX-4 and René CF6-80C2 HPT shrouds, there were also some CF6-80C2 shrouds for which the corrosion product did not contain sulphides (i.e. these shrouds were attacked by oxidation). For example, the two shrouds shown on the left of Fig. 11 were found to be attacked by hot corrosion while the two shrouds on the right of Fig. 11 were attacked by oxidation. It seems that this different degradation mechanism also has an influence on the discoloration pattern at the gas path surface. The two shrouds that were attacked by hot corrosion had a more “greenish” appearance also in the areas away from the rub area. On the other hand, for the shrouds attacked by oxidation, the corrosion product had a “greyish” appearance. Moreover, further away from the rub area, these shrouds appeared to be virtually free of environmental attack (i.e. they had a metallic appearance).

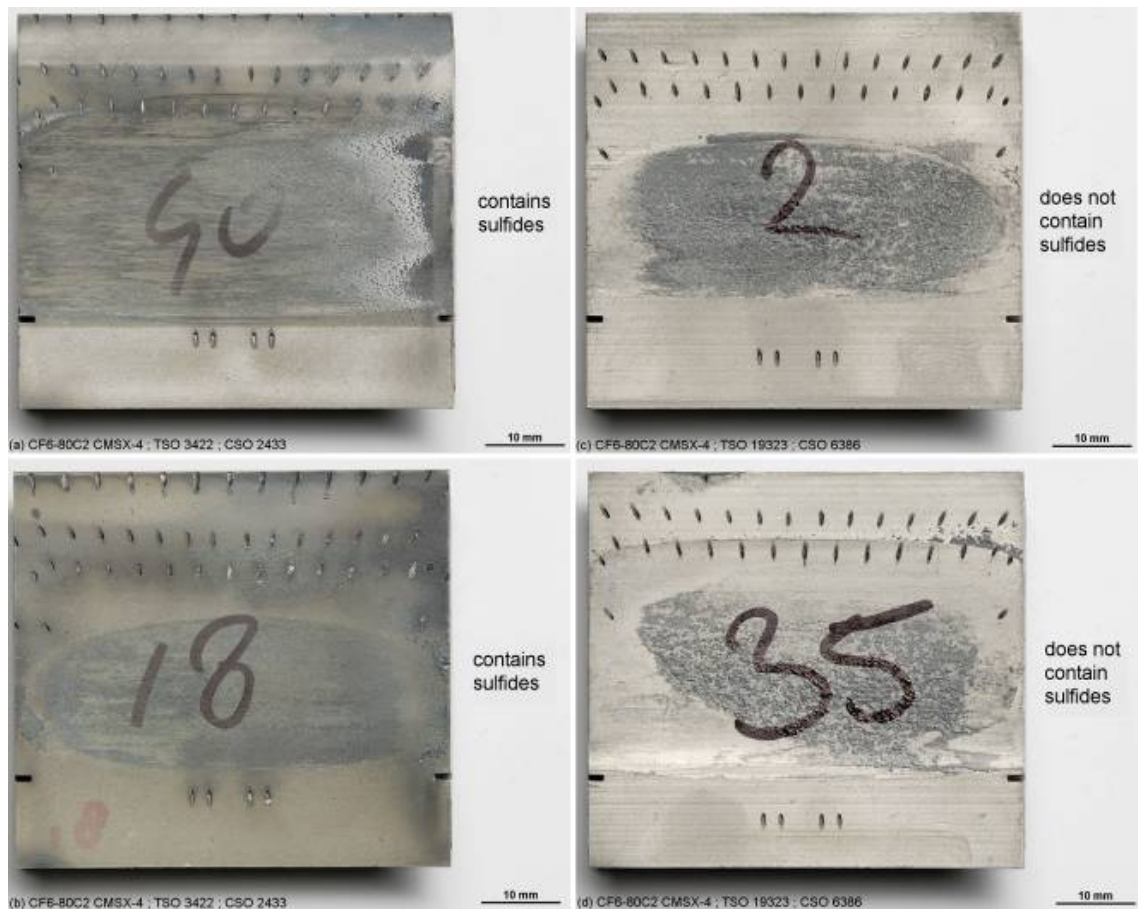


*Fig. 11: Macrographs of four 1<sup>st</sup> stage CMSX-4 CF6-80 C2 HPT shrouds. The two shrouds on the left originate from the same engine. This applies also for the two shrouds shown on the right.*

As an exception to the general damage pattern, occasionally 1<sup>st</sup> stage CF6-80C2 HPT shrouds which are severely attacked at the gas path surface are delivered to Chromalloy. An example of such a shroud is shown in Fig. 13. Clearly, the corrosion product covers the entire shroud surface and contains many ridges and craters, indicating that during service a significant amount of the corrosion product was already removed by means of spallation or rubbing. The corrosion product consisted of an outer layer of Ni rich oxide, an intermediate layer of Ta, W, Re and Al oxides and a region of Cr rich sulphide particles just below the corrosion product, similar to what was observed in Fig. 12c. However, instead of a continuous alumina layer the lower part of the corrosion product was made up of isolated Cr and Al rich oxides. Such a corrosion product is representative of a type I hot corrosion reaction that has extended into its (fast) propagation phase. Similar corrosion products as the one shown in Fig. 13 have also been detected in 1<sup>st</sup> stage CMSX-4 HPT shrouds in a LM6000 aero derivative engine that was operated in a coastal environment.

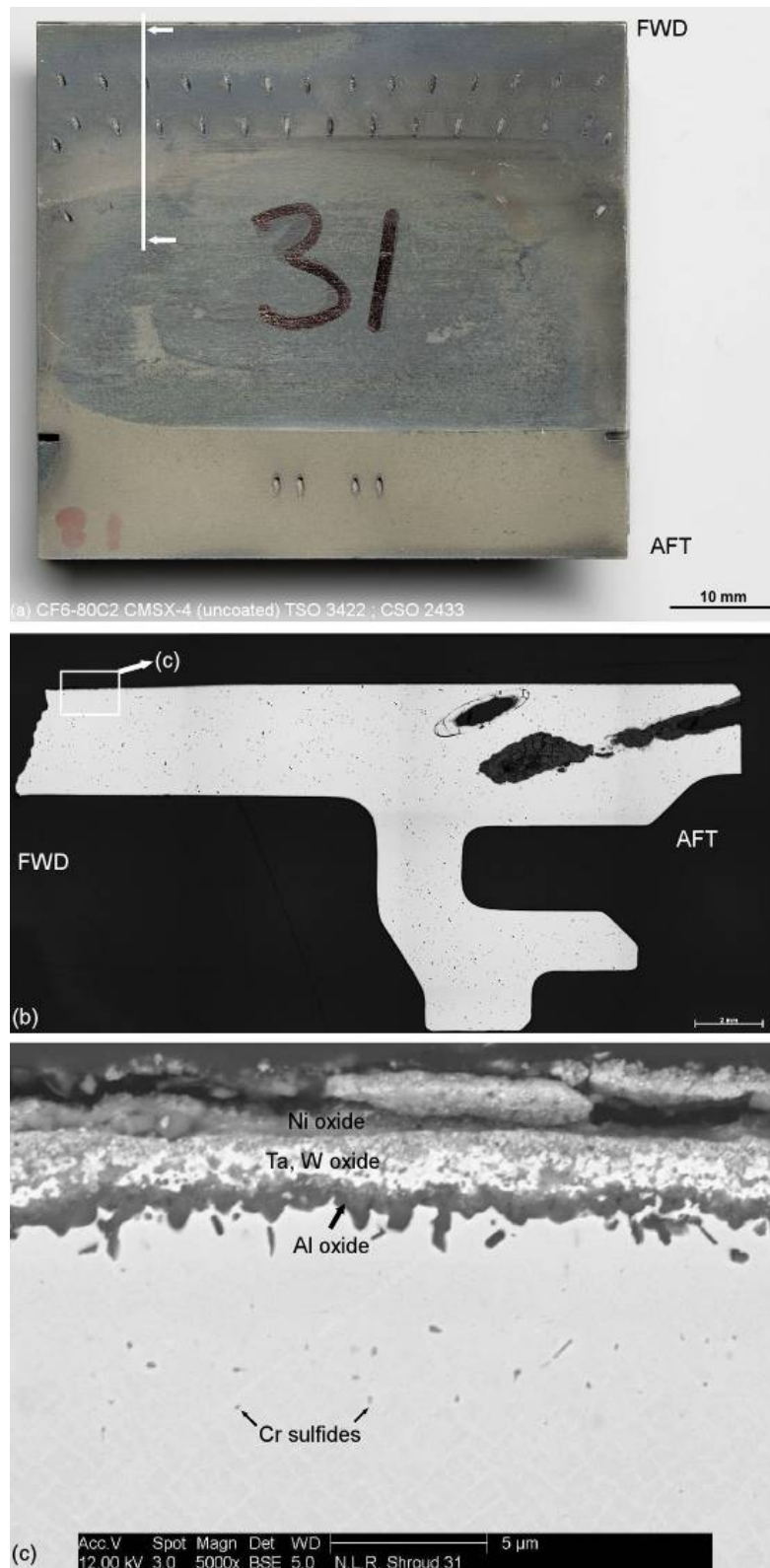


Fig. 12: (a) Surface macrograph, (b) optical micrograph of the cross-section indicated in (a) and (c) optical micrograph of the corrosion product and the location indicated in (b) of an ex-service 1<sup>st</sup> stage CMSX-4 CF6-80C2 HPT shroud.

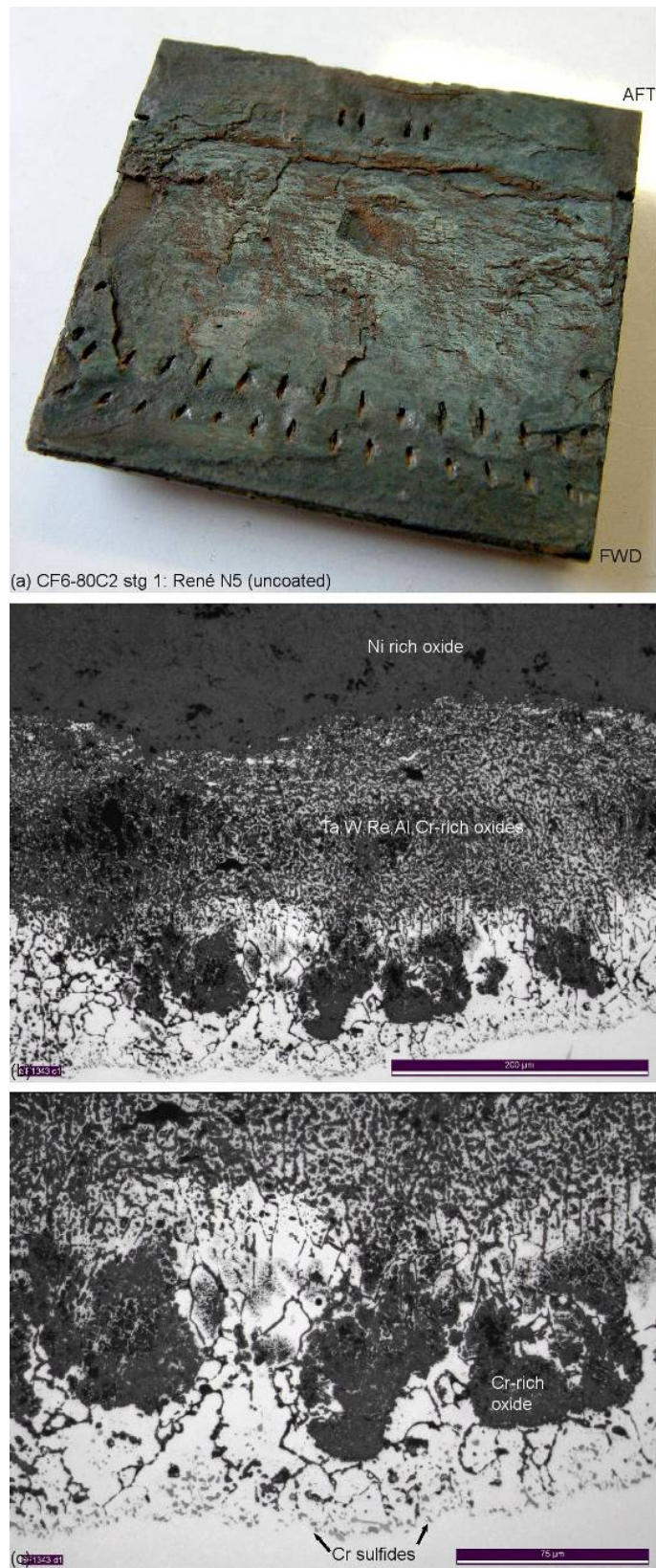


Fig. 13: (a) Surface macrograph, and (b,c) optical micrographs of the corrosion product for an ex-service 1<sup>st</sup> stage René N5 CF6-80C2 HPT shroud.

### 3.3 N2 CF6-50 shrouds

HPT shrouds made from the single crystal superalloy N2 have only recently been introduced by the OEM. However, several sets of deteriorated 1<sup>st</sup> stage CF6-50 N2 shrouds have already been sent to Chromalloy for repair. Such shrouds show macroscopic signs of severe environmental attack. This attack seems to be concentrated mostly near the edges of the shroud's gas path surface (Figs. 14a and b), but in some shrouds almost the entire gas path surface is attacked (Fig. 14c). As can be seen from one of the side surfaces of a N2 shroud (Fig. 14d), the environmental attack consumes a significant part of the original thickness of the shroud.

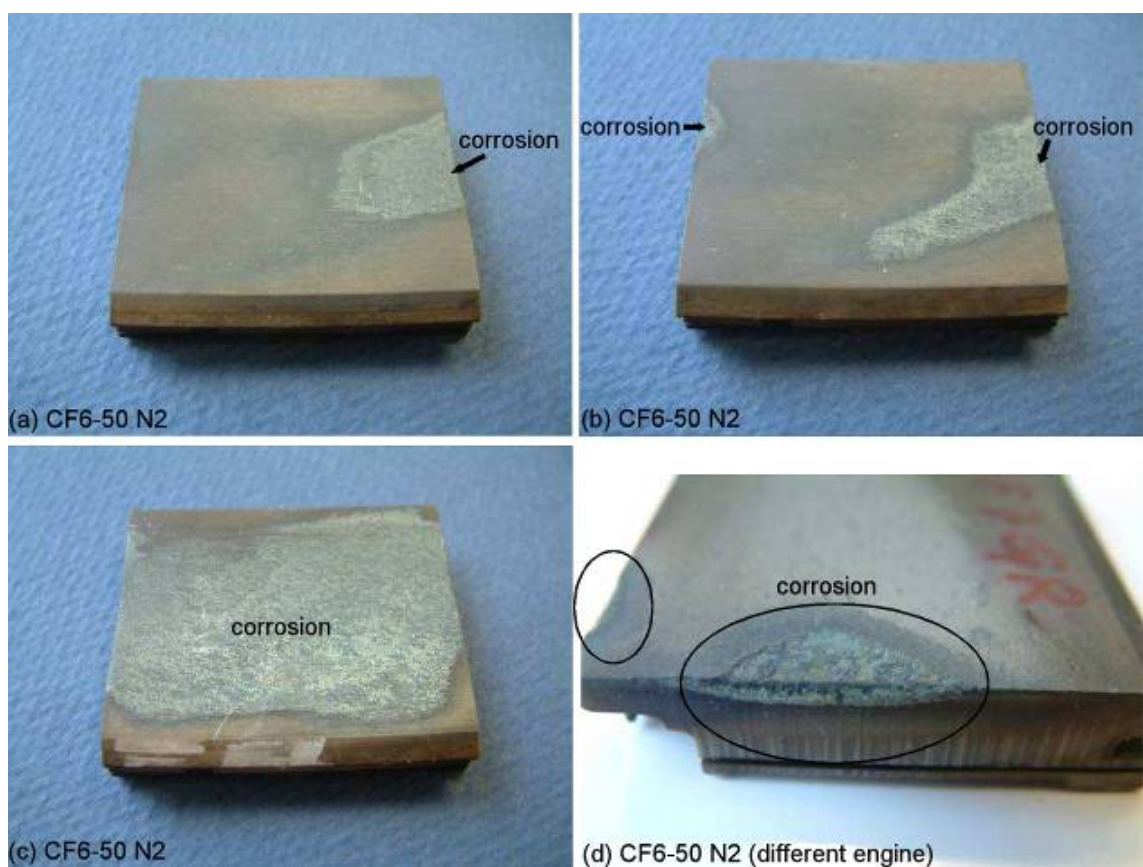


Fig. 14: Macrographs of four 1<sup>st</sup> stage N2 CF6-50 shrouds. The three shrouds with the blue background originate from the same engine. The circles highlight areas of severe environmental attack.

A cross-section through one of the shrouds revealed the presence of a thick corrosion product (more than 200  $\mu\text{m}$ ) which consisted of a porous outer layer and an inner layer containing isolated oxides (Fig. 15). Again, just below the corrosion product an array of small particles can be observed, which hints at the presence of sulphides (an EDS analysis to confirm this has not yet been executed). Therefore, this indicates that (1) the N2 CF6-50 shrouds were attacked by type I hot corrosion and (2) the corrosion reaction takes place at a relatively fast rate (indicating

that the propagation phase of hot corrosion reaction was already reached for these shrouds). This finding is surprising since the N2 patent [3] and the property data for N2 generated for this paper (Figs. 3-6) indicate that N2 was primarily introduced for its hot corrosion resistance. A similar degree of environmental attack is not observed for CoNiCrAlY coated 1<sup>st</sup> stage CF6-50 MAR-M509 HPT shrouds. This is in agreement with the hot corrosion laboratory test (Fig. 6), in which it was shown that Chromalloy's HVOF rub coating has a superior hot corrosion resistance over N2. Apparently, the improvement in the hot corrosion resistance of N2 over René N5 is not sufficient to prevent it from degrading by hot corrosion in some CF6-50 engines.



*Fig. 15: (a) Surface macrograph and (b) scanning electron micrograph of the corrosion product in an ex-service 1<sup>st</sup> stage N2 CF6-50 HPT shroud. The circles highlight areas where (sulphide) particles are visible below the corrosion product.*

### 3.4 René N5 shrouds with TDC coating

In comparison to uncoated single crystal superalloy shrouds, relatively little information has yet been obtained for single crystal superalloy shrouds with an external rub coating. For CFM56-5C HPT shrouds, the shrouds with an external rub coating seem to be less prone to environmental attack (i.e. oxidation) than the uncoated shrouds. As is shown in Fig. 16c and Figs. 17a and b, for most shrouds the coating surface shows almost no sign of discoloration even in areas where rub traces can be clearly detected. However, occasionally, CFM56-5C shrouds with a greenish appearance are observed (see Figs. 16a and b). It is seen that for these shrouds two additional rows of cooling holes have penetrated the gas path surface (Fig. 16b). By comparison of Fig. 1 and Fig. 16b, it is clear that these are the forward face cooling holes and the left side surface cooling holes, respectively. Normally, these cooling holes should not be visible at the gas path surface. This implies that the discoloured shrouds shown in Fig. 16a are significantly thinner than the shrouds that were not discoloured. This implies that either a significant erosion (e.g. by rubbing) of the rub coating has taken place or that these shrouds were excessively ground prior to service introduction (some airliners ground their shrouds to their own specified dimensions prior to engine assembly).

Most ex-service René N5 CFM56-5C shrouds with TDC rub coat examined so far are cracked and/or show signs of coating spallation (in particular near corners and edges; see Figs. 17b). Cracks are preferentially formed near cooling holes (not only near the cooling holes at the gas path surface but also near the cooling holes from the forward face and the left side surface, Fig. 17a). In addition, for some shrouds an additional mud-like crack pattern can be detected at the gas path surface behind the second row of cooling holes. The cracks near the cooling holes are more easily explained since finite element calculations show that at these locations the highest principle tensile stresses occur. In this respect it is noted that the CoNiCrAlY rub coatings are very thick ( $> 1$  mm), i.e. much thicker than the MCrAlY coatings normally employed on turbine blades ( $\sim 150$   $\mu\text{m}$  thick). In such thick coatings, cracking and spallation is more easily promoted, in particular if thermal expansion differences exist between the coating material and the single crystal superalloy substrate. An explanation for the mud-like cracking pattern behind the second row of cooling holes is currently lacking, but the formation of these cracks may be associated with rubbing (Fig. 17a).

1<sup>st</sup> stage René N5 CF6-80C2 HPT shrouds with a TDC rub coat show similar crack patterns as those observed for René N5 CFM56-5C shrouds with a TDC rub coat (Figs. 17c and d). However, apart from the cracking, the rub coat surface in the CF6-80C2 shrouds also seems to be attacked by oxidation and or corrosion (as apparent from the greenish discoloration at the surface of these shrouds in the rub area). Since no cross-sections have yet been prepared for

these shrouds, the extent and type of corrosion for these shrouds with rub coatings has not yet been established.



*Fig. 16: surface macrographs of ex-service René N5 CFM56-5C HPT shrouds with an external TDC rub coating. The circles highlight areas where the forward face and the left side segment cooling holes penetrate into the gas path surface of the shroud.*



Fig. 17: Surface macrographs of ex-service René N5 shrouds with an external TDC rub coating. (a,b) CFM56-5C HPT shrouds; (c,d) 1<sup>st</sup> stage CF6-80C2 HPT shrouds.

## 4 Discussion

From the results presented in Sec. 3 it is clear that the principal modes of visible degradation for uncoated single crystal superalloy HPT shrouds are oxidation or type I hot corrosion. Normally, the rate of oxidation increases with temperature and becomes only significantly high at temperatures above 1000 °C. On the other hand, type I hot corrosion degradation is most severe at lower temperatures of around 900 °C [9]. This indicates that, from the type of environmental attack observed in the shrouds, a relative ranking of the turbine inlet temperatures (TIT) for different engines can be derived. Of course, caution should be employed when making such an analysis, since hot corrosion is influenced by many other factors (e.g. the presence or absence of sea salt, the cleanliness of the fuel, etc.). In CFM56-5C engines, oxidation (accelerated by rubbing) seems to be the main mode of environmental attack. This indicates that the CFM56-5C engines operate at a relatively high TIT. The materials selection for the shrouds in this engine seems to substantiate this, since only the strongest single crystal superalloys are used for the

shrouds in this engine (CMSX-4 and René N5, see Fig. 3). In the CF6-50 engines, hot corrosion seems to be the most prominent degradation mode. Hence, this engine is expected to operate at a much lower TIT than the CFM56-5C engine (it is also a much older engine). Therefore, for the CF6-50 engine, it is not required to use the single crystal superalloys with the highest mechanical temperature capabilities. However, it was shown that even a hot corrosion resistant superalloy such as N2 does not seem to offer adequate corrosion protection for the shrouds of the CF6-50 engine. One option may be to use a rub coating within this engine on both new and repaired shrouds, as is already currently being done for MAR/M509 shrouds. However, it was shown that the application of such a thick rub coating is not without problems, since the rub coatings can spall and crack. Once spalled or cracked, the rub coating may offer much less corrosion resistance because of preferential ingress of oxygen through these cracks into the underlying superalloy. Further investigations on HPT shrouds with a cracked rub coating could clarify this. For CF6-80C2 shrouds both oxidation and type I hot corrosion have been observed as forms of environmental attack, indicating that the shrouds within this engine experience temperatures that are on the border of the accelerated hot corrosion and accelerated oxidation regimes. Whether the shrouds in a particular CF6-80C2 engine experience oxidation or hot corrosion degradation may then be dependent on where the aircraft is operated (low altitude flights near coastal areas) or the cleanliness of the fuel.

Apart from visible damage, almost all investigated single crystal superalloy shrouds experienced non-visible damage in the form of microstructure degradation (Fig. 18). This microstructure degradation was either in the form of the coarsening of the original  $\gamma'$  cuboidal microstructure (Fig. 18a) or more severely by the formation of a plate-like  $\gamma'$  microstructure due to coarsening and coalescence of the original  $\gamma'$  cuboids (Fig. 18b). Strongly directional  $\gamma'$  coarsening (i.e. rafting), which is frequently observed as the main form of microstructure degradation in turbine blades, has not yet been detected within HPT shroud cross-sections. Particle coalescence has been observed in CMSX-4, René N5 and N2 shrouds in the CFM56-5C, CF6-80C2 and the CF6-50 engines, indicating that this is a common form of microstructure degradation in HPT shrouds. However, the microstructural degraded area is normally confined only to a small region just below the gas path surface. Further into the interior of the shroud, the original microstructure is retained (Fig. 18). Since the microstructural degraded area is relatively thin, it is usually removed away by grinding during repair.

Finally it is noted that so far, signs of visual mechanical degradation such as cracks are rarely observed for HPT shrouds (even for shrouds for which more than half of the shroud thickness is severely corroded). Occasionally, shrouds are returned for which material is missing near edges or corners, but this kind of damage may also result from foreign object impact events.

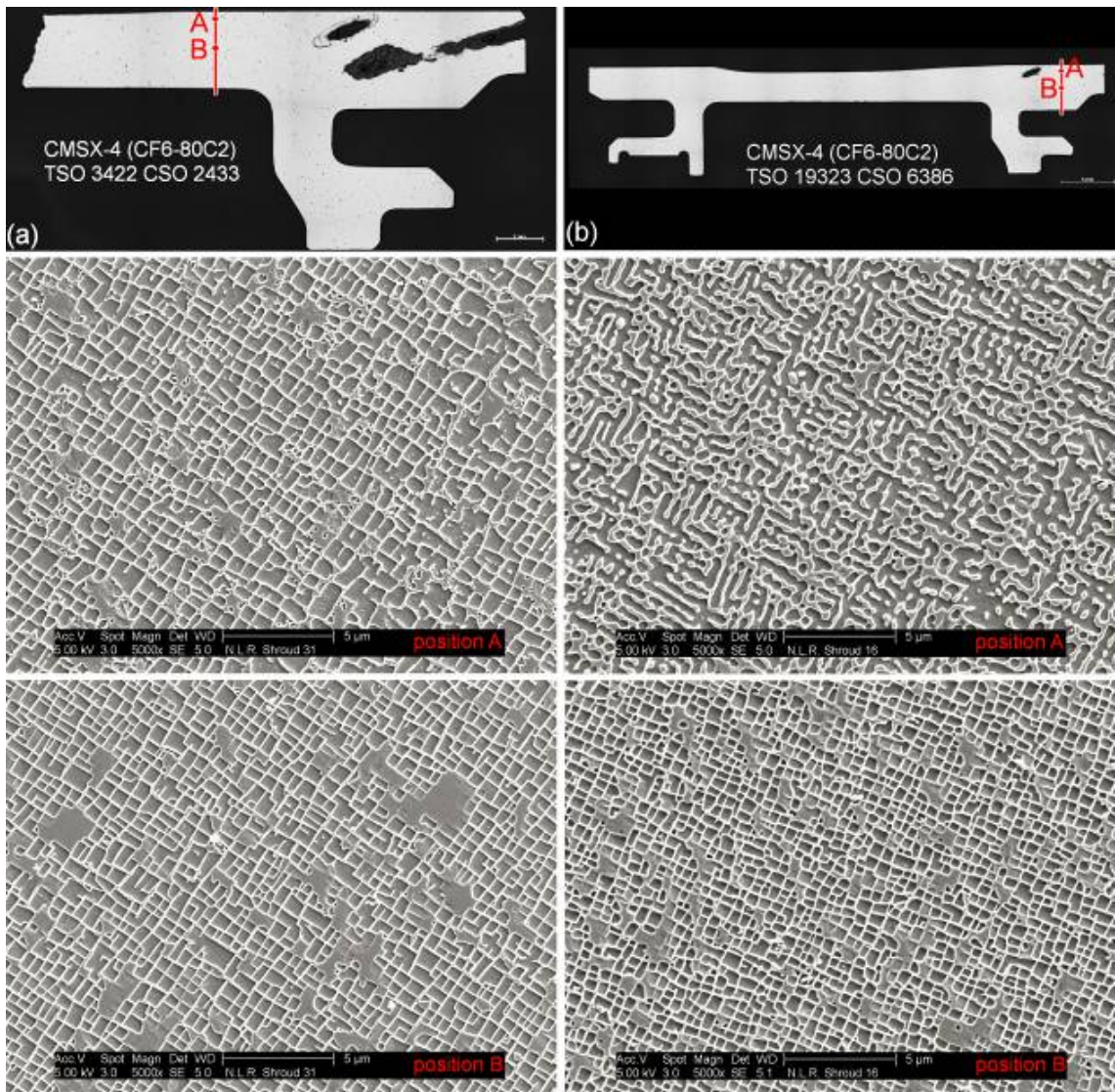


Fig. 18: Scanning electron micrographs of the microstructure in two ex-service CMSX-4 1st stage CF6-80C2 HPT shrouds at two positions (A) and (B) below the gas path surface.

## 5 Conclusions

- Uncoated single crystal superalloy HPT shrouds primarily degrade by environmental attack. Depending on the engine type, type I hot corrosion or oxidation accelerated by rubbing is the most dominant degradation mode.
- Single crystal CFM56-5C shrouds are primarily attacked by oxidation. However, severe oxidation attack only occurs when the shroud also experiences shroud-to-blade-tip rubbing. If no rubbing occurs during engine operation, the degree of oxidation attack is minimal.
- 1<sup>st</sup> stage single crystal superalloy shrouds for the CF6-80C2 engine either are attacked by oxidation or type I hot corrosion. In general, the degree of environmental attack for CF6-80C2 shrouds is much less than for the CFM56-5C shrouds and the CF6-50 shrouds.
- 1<sup>st</sup> stage CF6-50 shrouds made out of the single crystal superalloy N2 show severe environmental attack despite the fact that N2 has been specifically developed for optimum oxidation and hot corrosion resistance.
- Rub coatings that are applied during repair of single crystal superalloy HPT shrouds are less prone to environmental degradation, but are susceptible to cracking around cooling holes and coating spallation near corners and edges.

## Acknowledgements

The authors are indebted to Jan Mathijssen at Chromalloy Holland and Henk Kolkman, Rob Huls, Tim Hattenberg, Roland Diks, René Vermeulen, Hans Faber, Frank Hoekstra, Niels Wildeboer, Ton van de Belt and Gert Bos at NLR for providing valuable input for this paper. The Netherlands agency for aerospace research (NIVR; now incorporated into Agentschap NL) is acknowledged for sponsoring part of this work.

## References

- [1] *Metallurgy, processing and properties of superalloys*, in ASM specialty handbook heat resistant materials, J.R. Davis (editor), ASM international (1997) 221-254.
- [2] T. Khan, P. Caron, *Advanced superalloys for turbine blade and vane applications*, CIM symposium on advanced in gas turbine engine materials, Ottawa, Canada, August 19-20 (1991).
- [3] K.S. O'Hara, W.S. Walston, C.G. Mukira, M.R. Jackson, *Nickel-base superalloy composition and its use in single-crystal articles*, United States Patent 6,905,559 B2 (2005).
- [4] K.S. O'Hara, L.J. Carroll, *Low rhenium nickel base superalloy compositions and superalloy articles*, International patent application WO 2009/032578 A1.
- [5] P.A. Dasilva, D.E. Budinger, J.J. Reverman, *Repair of HPT shrouds with sintered preforms*, US patent 7,653,994 B2 (2010).
- [6] K.P.L. Fullagar, R.W. Broomfield, M. Hulands, K. Harris, G.L. Erickson, S.L. Sikkenga, *Aero engine test experience with CMSX-4 alloy single crystal turbine blades*, Journal of Engineering for gas turbines and power, 118 (1996) 380.
- [7] W.S. Walston, K.S. O'Hara, E.W. Ross, T.M. Pollock, W.H. Murphy, *René N6: third generation single crystal superalloy*, Proceedings of The Superalloys (1996) 27.
- [8] *Design for oxidation resistance*, in ASM specialty handbook heat resistant materials, J.R. Davis (editor), ASM international (1997) 534-547.
- [9] M.J. Donachie, S.J. Donachie. *Superalloys – a technical guide*, 2nd edition (2002) 287-322.
- [10] A. Epishin, T. Link, M. Nazmy, M. Staubli, H. Klingelhöffer, G. Nolze, *Microstructural degradation of CMSX-4: kinetics and effect on mechanical properties*, Proceedings of The Superalloys (2008) 725.